

proximately 5 dB. Of course, for fixed P_p , as β deviates from 1.1, the negative-resistance level will decrease slightly and make the matching problem to achieve a gain G at ω_s somewhat more difficult.

Another benefit of overdrive is in the fractional sensitivity of R_{in} to fractional variations in the pump power. Calculating this sensitivity gives

$$\sigma(\beta) = \frac{dR_{in}/R_{in}}{dP_p/P_p} \approx \frac{\beta \frac{dF(\beta)}{d\beta}}{F(\beta)}$$

$$= \begin{cases} \frac{\beta \sin^{-1} \frac{1}{\beta} - \sqrt{1 - (1/\beta^2)}}{\beta \sin^{-1} \frac{1}{\beta} + \sqrt{1 - (1/\beta^2)}}, & \beta < 1. \\ 1, & \beta > 1. \end{cases} \quad (37)$$

and a plot of $1/\sigma(\beta)$ is also indicated in Fig. 10 as a function of β . From the curves of Fig. 10 it is apparent

that substantial benefits in parametric amplifier performance are available by using Read-type or HI-LO varactors.

IV. CONCLUSIONS

It has been shown that the performance of parametric amplifiers can be improved in general and specifically by use of Read-type HI-LO varactors. Optimum values for doping levels and widths of the LO region and pump drive levels have been specified which optimize certain performance criteria when external limitations can be specified. As these diodes become more available, their use in parametric amplifiers will increase, particularly at millimeter-wave frequencies where pump power limitations and circuit losses are most severe.

REFERENCES

- [1] P. Penfield and R. P. Rafuse, *Varactor Applications*. Cambridge, MA: M.I.T. Press, 1962.
- [2] L. A. Blackwell and K. L. Kotzebue, *Semiconductor-Diode Parametric Amplifiers*. Englewood Cliffs, NJ: Prentice-Hall, 1961.

A 40-GHz Digital Distribution Radio with a Single Oscillator

MASAYASU HATA, MEMBER, IEEE, ATSUSHI FUKASAWA, MASAHIRO BESSHIO, SHOJI MAKINO, AND MICHIO HIGUCHI

Abstract—New 40-GHz band digital radio equipment is described. In the equipment we adopted a new circuit configuration consisting of a single IMPATT diode oscillator which functions as both transmitter frequency converter and receiver local oscillator simultaneously. The principal system design factors, a unique IMPATT diode oscillator mount configuration, and test results are described. The compact radio equipment is designed so that it ensures excellent cost performance for communication systems in local trunk service, even in short hop applications resulting from rainfall attenuation in the new band.

I. INTRODUCTION

IN INTRACITY and suburban areas, voice and data business communications are expanding rapidly. In such areas it is difficult to use buried cables, while there also exists the problem that the radio spectrum is very congested. Under these circumstances, in late 1974 the FCC

made the 40-GHz band available for such applications as local trunk service.

In this paper, newly developed 40-GHz digital radio equipment is described. For this radio equipment to be used in local trunk service, it must firstly be of low cost, since the channel loadings are small, i.e., up to 24 channels, and the radio span is only up to ten miles. Secondly, it must interface with the digital signal format, i.e., PCM, which is economically appropriate for a variety of signals such as voice, data, FAX, etc. Thirdly, it must be easy to install and maintain.

Considering the above requirements, we have successfully developed a unique transmitter-receiver configuration consisting of a single IMPATT diode oscillator which functions as transmitter oscillator, up converter, and receiver local oscillator simultaneously. As a result of this, we achieved considerable cost reduction while obtaining smaller size, lower power consumption, better reliability, and easier maintenance. The waveguide circuits, which

Manuscript received January 8, 1980; revised April 3, 1980.

The authors are with OKI Electric Industry Co., Ltd., 4-10-12 Shibaura Minato-ku, Tokyo, Japan, 108.

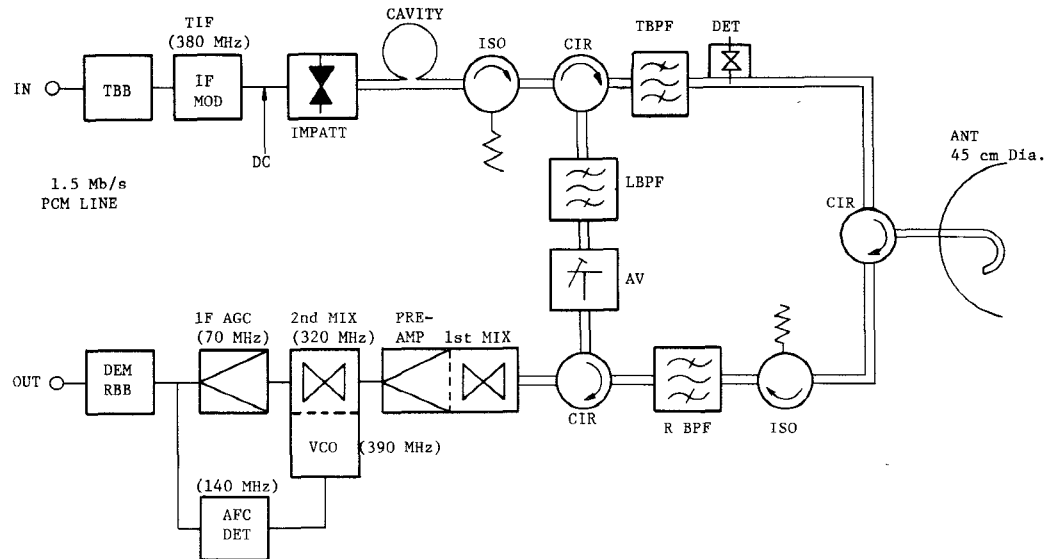


Fig. 1. Block diagram of single local oscillator transceiver.

are the most expensive part of such equipment, are reduced to about one half those of conventional equipment.

Moreover, we adopted a new IMPATT diode mount configuration in which the diode is soldered onto a stud and is directly screwed into the standard waveguide, reducing the mount cost and obtaining stable operation.

II. SINGLE OSCILLATOR TRANSCEIVER

A single oscillator transceiver is preferable from viewpoints of simplification and cost reduction of the equipment. In this paper, a unique single oscillator transceiver is described. The block diagram is shown in Fig. 1. The radio system uses biphase shift keying (PSK) modulation. The principal merit of PSK modulation is the better bit error rate (BER) characteristic as compared with that of FSK or ASK (Amplitude Shift Keying) modulation for a given received carrier-to-noise power ratio (C/N).

The biphase PSK signal $S(t)$ is expressed as

$$S(t) = A \cos \{ \omega t + [0 \text{ or } \pi] + \theta_0 \} \quad (1)$$

in which A , ω , and θ_0 are the amplitude, angular frequency, and initial phase of the signal, respectively. The term [0 or π] denotes the phase modulation, which depends on a binary code signal to be transmitted.

In the transmitting baseband unit (TBB) in Fig. 1, the incoming PCM signal of 1.544 Mbit/s is processed to give a pulse code signal appropriate for radio transmission. The principal functions are code conversion, differential logic operation, and nine-stage pseudo random code signal scrambling. The scrambling suppresses the generation of line spectrum which has strong power in the transmitted signal.

In the intermediate frequency modulator (IF MOD) shown in Fig. 1, a transmitting IF carrier signal of 380 MHz is biphase modulated by the code signal from the TBB. The output signal of the IF modulator is expressed as in (1). The signal is applied to a bias circuit of an IMPATT diode oscillator and modulates the magnitude of the current.

Although in an IMPATT diode the impedance can vary with dc current depending on the ratio of operating frequency to avalanche frequency, Greiling and Haddad [1] and others [2] have shown that the bias current variations in an IMPATT diode mainly change the conductance of the diode and that the device susceptance variation is relatively small well above the avalanche frequency. Accordingly, the output signal of the IMPATT diode oscillator is amplitude modulated by the transmitting IF signal. Three output signals (f_L , f_T , f_S), therefore, come from the IMPATT diode oscillator, as shown in Fig. 2. One is the original oscillating signal (f_L) and the other two signals (f_T and f_S) are the upper and lower sidebands due to the amplitude modulation. These two sidebands, f_T and f_S , are, respectively, separated by $T_{IF} = 380$ MHz from the oscillating signal f_L . The upper sideband in this case as shown in Fig. 2, is utilized as a transmitting signal passing through the T BPF filter. The lower sideband and other higher order converted signals are reflected from both the L BPF and T BPF filters and then absorbed by the isolator.

On the other hand, oscillating signal f_L , of which the frequency is stabilized by means of a reflection high Q cavity, is fed to the first mixer as a local signal through L BPF and attenuator AV . The local signal is a continuous wave without modulation.

The transmitting and receiving frequencies of the radio system are in accordance with FCC regulations. The regulations, Docket No. 18920 issued late in 1974, assign the 14 both-way (28) RF channels between 38.6 and 40 GHz, as shown in Fig. 3. Each channel has a bandwidth of 50 MHz, and the channel separation for a pair of transmitting and receiving frequencies is 700 MHz. The frequencies are so arranged that the first IF frequency of the single oscillator transceiver is $R_{IF} = 320$ MHz ($= 700 - T_{IF}$) as shown in Fig. 2.

In the receiver, the received signal is converted to the first IF signal of 320 MHz and then to a second IF signal of 70 MHz. In the second mixer, a transistorized voltage

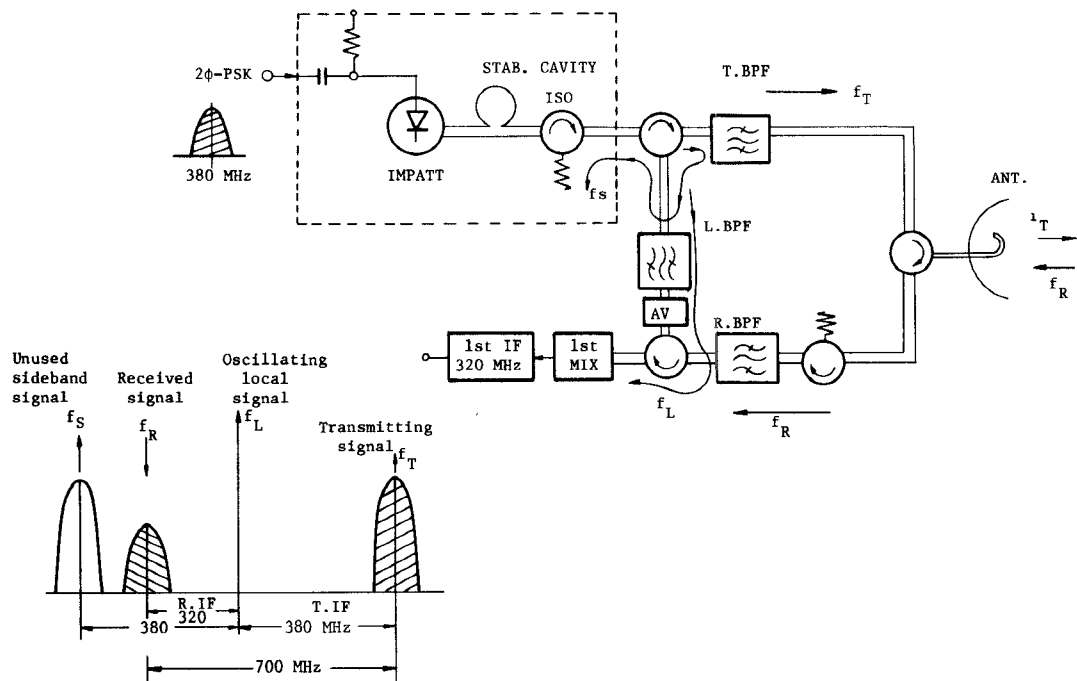


Fig. 2. Frequency relations between transmitter and receiver.

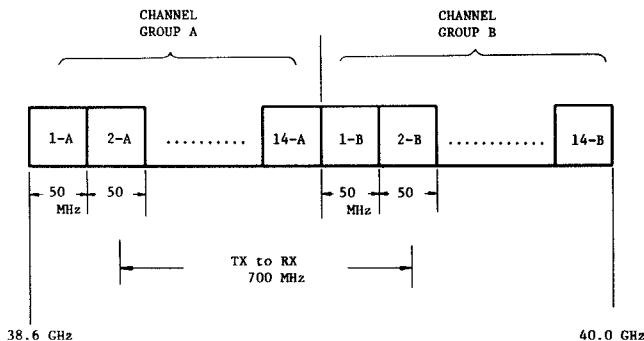


Fig. 3. FCC channel plan.

controlled oscillator (VCO) of 390 MHz serves as the local source to which an AFC signal of about the second IF frequency is fed back.

The frequency stability of the IMPATT diode oscillator obtained is about 0.012 percent for a temperature range of -20 to $+60^\circ\text{C}$, and for two IMPATT diode oscillators of two adjacent stations the frequency variation in the worst case comes to 9.6 MHz. However, the preferred receiver bandwidth for PSK modulation to obtain a better BER is approximately equal to the clock frequency of 1.544 MHz. In order that such a narrow-band IF filter can be used, the frequency variation of the second IF signal is reduced to about 100 kHz by the AFC configuration.

The direct frequency discrimination of the PSK signal modulated by a random code sequence, however, gives no frequency information, since the signal has no stationary carrier components. Therefore, the second IF signal of 70 MHz is frequency multiplied to a signal without phase modulation. The frequency multiplied signal of (1) becomes

$$S_d(t) = B \cos \{2\omega t + 2[0 \text{ or } \pi] + 2\theta_0\} \quad (2)$$

in which B is the amplitude and the argument of the signal (2) is a doubled replica of that of the signal (1). The phase modulation term $2[0 \text{ or } \pi]$, therefore, comes to a value independent of the phase modulation.

The demodulator unit (DEM) demodulates the IF signal to a baseband pulse code signal by means of synchronous detection. After the detection, in the receiving baseband unit (RBB) the detected pulse code signal is regenerated through polarity decision, retiming, and reshaping in the usual way. Then the descrambling and logical sum, which are the reverse of the operations which take place in the transmitter, take place in the unit. The resulting received PCM signal is then sent to a pair of cables in the form of a normal bipolar signal.

III. IMPATT DIODE OSCILLATOR

A. Diode Mount Configuration

A unique IMPATT diode oscillator with a simple diode mount was developed with the criteria of stable operation with a wide range of working conditions [3]. Fig. 4 shows a schematic diagram of the IMPATT diode oscillator. The IMPATT diode with a soldered disk hat resonator is mounted on a stud and the stud is simply screwed into a brass block forming a part of the waveguide of WRJ-320 (WR-28). A biasing post or circuit of the IMPATT diode sometimes creates difficult implementation problems in circuit and mechanical designs. In the mount, a biasing lead wire passed through a tiny hole in the stud to the outside. With this configuration eliminating a complex impedance characteristic which often causes spurious oscillation and frequency jumping of the oscillator, we developed a stable and cost-effective IMPATT diode oscillator. Recently, a similar configuration, called a "pre-tuned module," was reported [4].

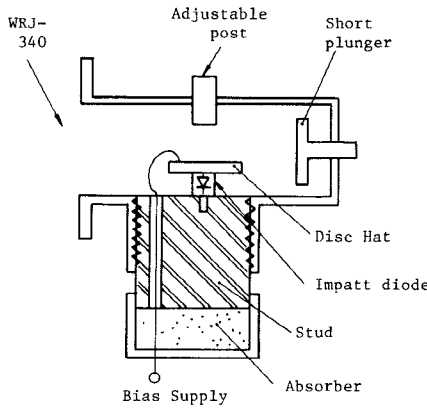


Fig. 4. Schematic diagram of hat-type IMPATT diode oscillator.

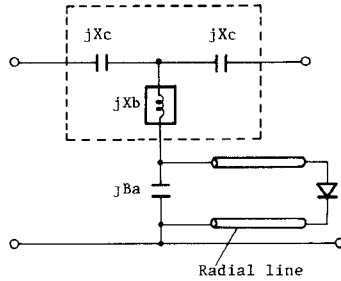


Fig. 5. Equivalent circuit of radial line resonance.

The frequency of the IMPATT diode oscillator is primarily determined by the radial line resonance of the disk hat attached to the diode. The electric field at the edge of the hat couples with the dominant mode of rectangular waveguide WRJ-320.

An equivalent circuit of the oscillator with the hat is shown in Fig. 5 [5], [6]. The hat is regarded as a post projected into the waveguide. In the case of a fine post, the coupling between the post and the waveguide is represented by the T circuit consisting of jX_c and jX_b enclosed by a dotted line. An adjustable post on the other side of the waveguide wall can adjust the amount of coupling at the given frequency, and the equivalent circuit is contained in the same T circuit of the Fig. 5. Susceptance jB_a stands for the electric field concentration near the edge of the hat.

The IMPATT diode is OKI's TX-40 and is the silicon single drift region type of approximately $60\text{-}\mu$ junction diameter. It has minimum output power of 200 mW with efficiency of 5.5 to 7.5 percent. The typical operating bias voltage and current are 29 V and 100 mA, respectively. Fig. 6 shows the diode package of minidisk type and the typical characteristics of the IMPATT diode.

Fig. 7 shows the diode stud. The disk hat soldered onto the top of the diode package is of copper plate of 0.1-mm thickness and about 3-mm diameter and the gap between the hat and the stud is about 0.15 mm. An insulated lead wire for power supply passes through a hole in the stud. The bias lead wire inside the waveguide is a fine copper wire of 0.16-mm diameter and about 1.5-mm length. It has

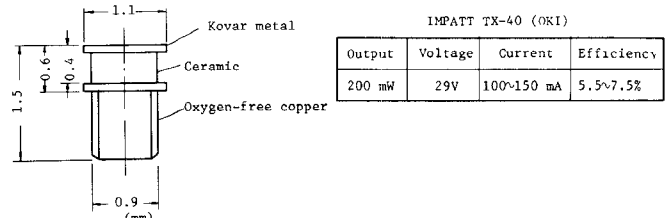


Fig. 6. IMPATT diode package and characteristics.

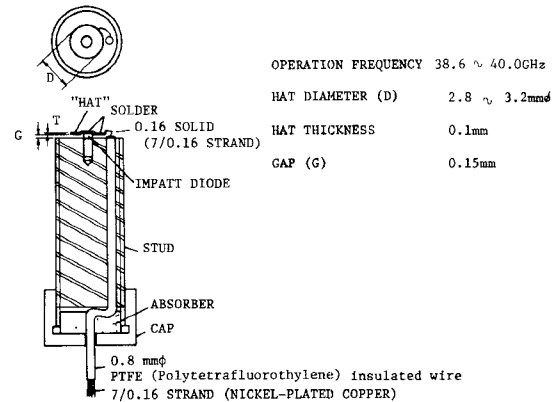


Fig. 7. Diode stud with a disk hat resonator.

sufficiently high impedance to separate the bias circuit at the oscillating frequency. It is, of course, kept away from the strong electric field in the vicinity of the edge of the hat resonator. Although a static capacitor formed between the insulated lead wire and the wall of the stud hole reduces leakage of RF energy, a microwave absorber of disk type made of "epo-iron" is provided at the outer end of the stud to ensure more complete suppression of RF leakage and suppress reactions from the bias circuit on the power and frequency of the oscillator.

Fig. 8 shows the output power and the frequency versus bias current of the IMPATT diode oscillator. The figure shows the data for two kinds of radial hat: hat no. 1 ($D=3.1$ mm, $t=0.1$ mm, $G=0.15$ mm), and hat no. 2 ($D=3.4$ mm, $t=0.6$ mm, $G=0.15$ mm). For hat no. 1 the dotted curve shows results when the position of the short plunger is fixed. For hat no. 1 the solid curve shows results when the position of the plunger is adjusted to set the frequency at 40.05 GHz for each bias current. The curves shown for hat no. 2 indicate the situation for fixed plunger position.

Although the oscillating frequency is determined by the dimensions of the disk hat, and especially the diameter thereof, the value of the junction capacitor varies from diode to diode and requires a hat diameter differing by 0.2–0.3 mm for a given oscillating frequency of each diode. The gap of the hat and the position of the plunger of the oscillator are the principal factors permitting adjustment of the oscillating frequency of a given hat.

Fig. 9 shows the changes of the output power and frequency of the oscillator when the gap from the disk hat to the waveguide is varied by rotating the screw-in stud.

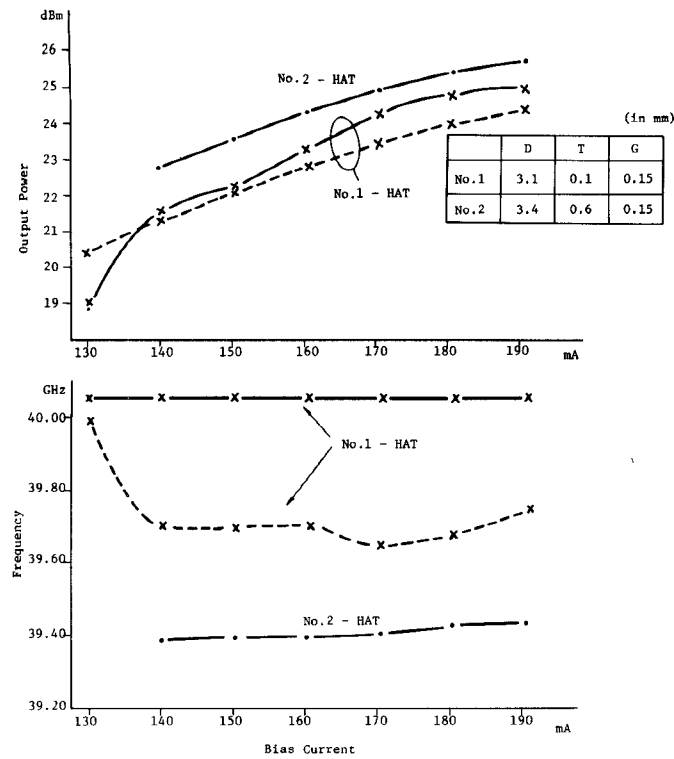


Fig. 8. Output power and frequency versus bias current for no. 1 and no. 2 hats.

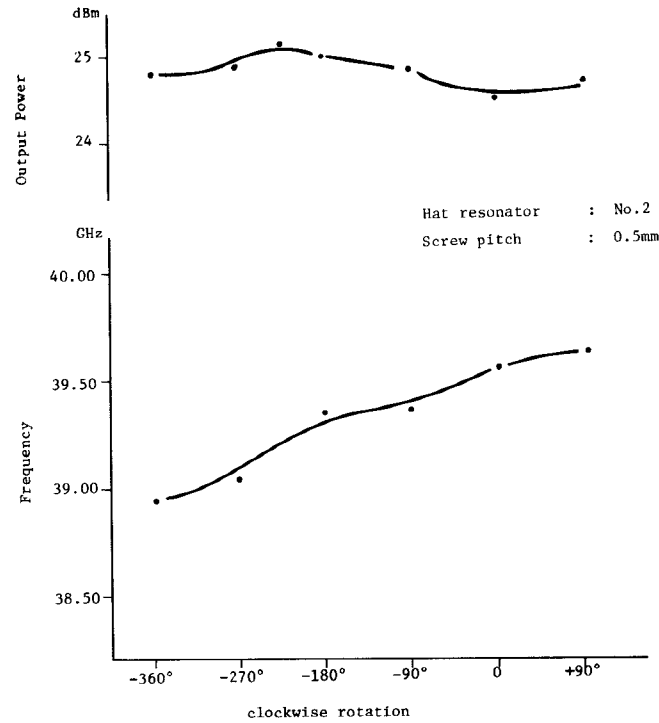


Fig. 9. Relation of oscillating output power and frequency to hat gap when diode stud is rotated.

The frequency changes by about 500 MHz per full rotation. The pitch of the thread of the screw-in stud is 0.5 mm.

Fig. 10 shows the variation of frequency (ordinate) and output power (abscissa) when the plunger position is varied

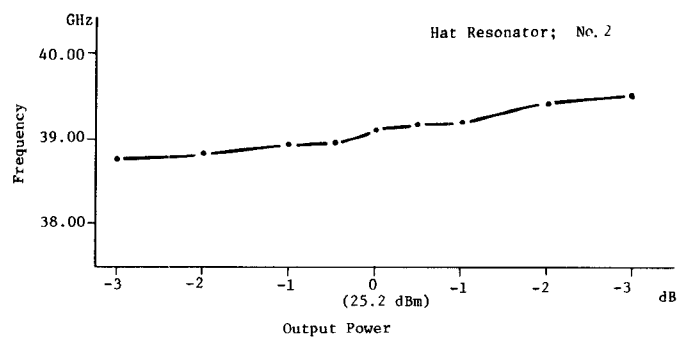


Fig. 10. Frequency and output power as the plunger position is varied from maximum output position.

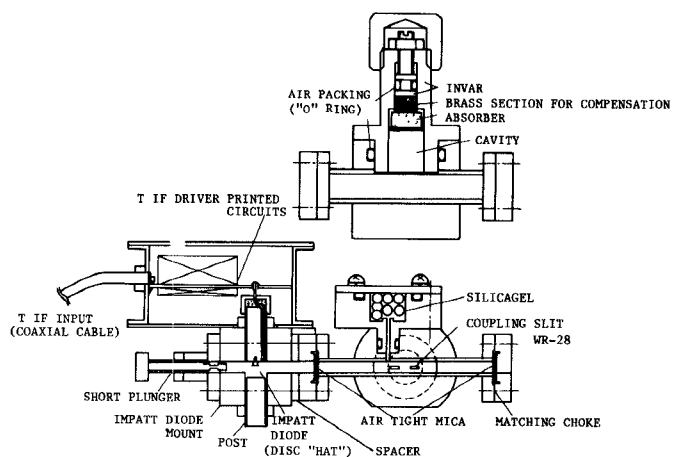


Fig. 11. IMPATT diode oscillator with stabilizing cavity.

from the position of the maximum output power ($= 25.2$ dBm) at the frequency of 39.10 GHz

B. Frequency Stabilization of IMPATT Diode Oscillator

Frequency stabilization of the IMPATT diode oscillator is achieved by means of a reflecting high Q cavity [7], [8]. Fig. 11 shows the mechanical details of the cavity-stabilized oscillator. In the figure, the oscillator is followed by a frequency stabilizing cavity. Part of the output power of the original oscillator is reflected from the cavity and then injected into the original oscillator. The resulting equivalent load susceptance represented by the reflected wave adds to the susceptance of the original oscillator. When any change in the susceptance of the original oscillator is effected by some cause, it is cancelled by the susceptance variation of the same amount caused by the stabilizing cavity in response to the slight variation of frequency of the stabilized oscillator, since the total susceptance should be zero.

Since frequency sensitivity $\partial B / \partial \omega$ of susceptance B represented by the stabilizing cavity is much higher than that of the original oscillator, the resulting frequency variation is greatly decreased or made negligible as compare with that of the original oscillator.

The cavity is made of invar iron with expansion coefficient of about $10^{-6} / ^\circ\text{C}$ and, furthermore is temperature compensated by provision of a brass section in the tuning

piston. The cavity is silverplated to a thickness of 4~5 μm . The unloaded Q is about 12 000 in the 40-GHz band. The cavity is hermetically sealed with a mica plate on both end flanges and it contains silica gel on the reverse side of the tuning rod, as shown in Fig. 11, to prevent the tuning frequency from drifting because of alteration of the dielectric constant by moisture entering into the cavity. The condition of the silica gel can be monitored through a small window provided for maintenance.

The electrical angle between the oscillator and the cavity determines the stabilization characteristics, and the angle is adjusted by a spacer of adequate thickness as indicated in the next paragraph.

IV. SINGLE OSCILLATOR TRANSCEIVER

A. Bias Modulation and Frequency Stabilization

The frequency conversion characteristics in the IMPATT diode oscillator were studied by Evans and Haddad [9] and others. As regards the design of this single oscillator transceiver, it is important to make clear the mutual relations between the frequency stabilization and the frequency conversion characteristics of the IMPATT diode self-oscillating frequency converter.

Shirahata *et al.* [7] have analyzed the frequency stabilization of an oscillator with a band rejection filter. On the other hand, Shiota *et al.* [10] have discussed frequency conversion in the case of stabilized solid state oscillators with the aforementioned reflection high Q cavity.

Referring to the above mentioned papers, we next discuss whether the bias modulation degrades the frequency stability and whether the stabilizing cavity distorts the modulation signal, since the IMPATT diode oscillator, in this radio system, functions as receiver local source as well as frequency converter and transmitting local oscillator.

Fig. 12 shows the bias modulation circuit for the IMPATT diode oscillator. Fig. 13 shows a simplified equivalent circuit of the IMPATT diode oscillator with the frequency stabilization cavity. The negative conductance \tilde{G} of the IMPATT diode varies in accordance with the bias current. In the equivalent circuit, the radial line resonance circuit is shown as a single tuning circuit of L_1 and C_1 . Q_1 denotes the external Q of the IMPATT diode oscillator, where $Q_1 = \omega_1 C_1 / Y_0$ and Y_0 is the load admittance.

The stabilizing cavity is denoted by a parallel resonance circuit of L_2 , C_2 , and R_2 , which is connected in series to the original oscillator through a line of electric angle θ , where Q_2 and f_2 are unloaded Q and the resonant frequency of the stabilizing cavity, respectively.

The coefficient of the coupling of the cavity to the load is given by $R_0 Y_0$, and S denotes the VSWR which measures load Y_0 seen through the cavity at resonant frequency f_2 .

The electrical angle θ is adjusted to $\theta=0$ or $2n\pi$ (n integer) by selecting the spacer between the diode mount and the stabilizing cavity in order to obtain proper frequency locking characteristics. The phase lag is negligi-

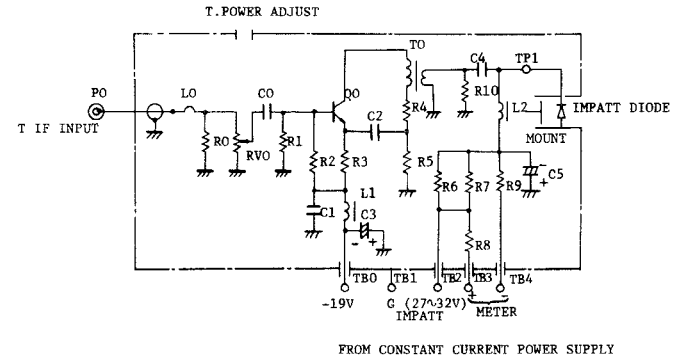


Fig. 12. Bias modulation circuit for IMPATT diode oscillator.

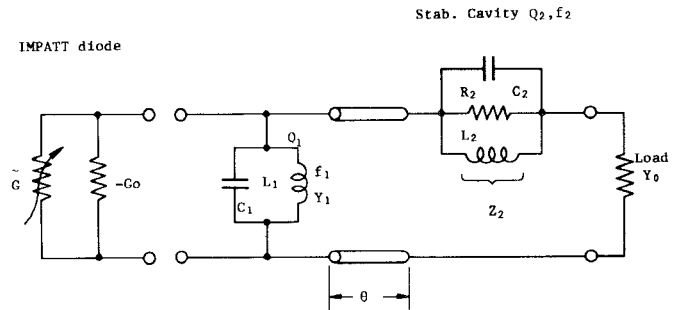


Fig. 13. Equivalent circuit of frequency-stabilized IMPATT diode oscillator with bias current modulation.

ble against the phase given by the stabilizing high Q cavity, since the integer n is selected as low as possible in order to get a wide frequency locking bandwidth.

The external Q of the frequency stabilized oscillator in the case of $\theta=0$ or $2n\pi$ is approximated by the following expression:

$$Ex Q \approx \frac{S-1}{S^2} Q_2 \quad (3)$$

and the maximum insertion loss L introduced by the stabilizing cavity is given by [7]

$$L = \frac{(1+S)^2}{4}. \quad (4)$$

The values for this equipment are as follows:

$$Q_1 = \omega_1 C_1 / Y_0 = 25$$

$$Q_2 = \omega_2 C_2 R_2 = 12\,000$$

$$S = R_0 Y_0 + 1 = 2$$

$$Ex Q \approx \frac{S-1}{S^2} Q_2 = 3000$$

$$L \approx \frac{(1+S)^2}{4} = 3.5 \text{ dB}.$$

Fig. 14 shows a simplified frequency locking characteristic when the free running frequency f_1 of the original oscillator is varied. The output frequency f_3 of the cavity-

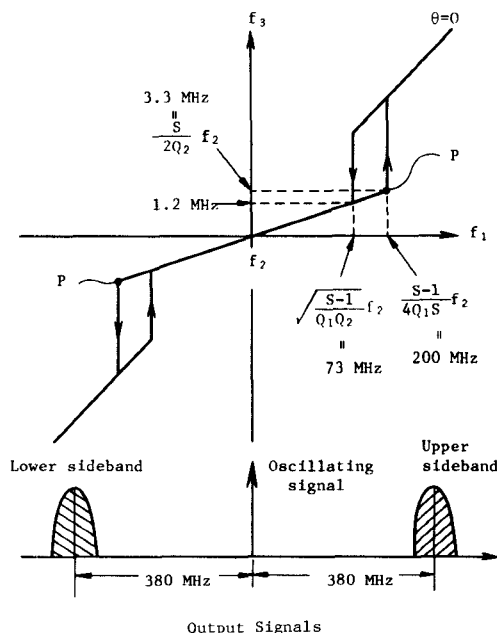


Fig. 14. Simplified frequency locking characteristics of oscillator with stabilizing high Q cavity ($\theta=0$). The lower figure shows the frequency relation of the output signals of the IMPATT diode oscillator with bias modulation.

stabilized oscillator indicates a well-known hysteresis curve. The pull-in range of the stabilized oscillator is given by the equation

$$f_2 \pm \sqrt{\frac{S-1}{Q_1 Q_2}} f_2. \quad (5)$$

For the parameters given above, the pull-in range is 146 MHz (± 73 MHz) as shown in Fig. 14.

On the other hand, the original unstabilized IMPATT diode oscillator varies about 120 MHz in frequency over the temperature range of -20°C to 60°C and the variation, therefore, is within the pull-in range.

Fig. 15 shows stable frequency versus ambient temperature for the cavity stabilized IMPATT diode oscillator. The frequency of the 40-GHz band signal was measured by using frequency counter system HP E80-5245L.

Experimentally, the frequency variation of the stabilized oscillator over the temperature range of -20°C to $+60^{\circ}\text{C}$ was 1.6 MHz. On the other hand, the estimated frequency variation from the analysis is given as follows. The frequencies of jumping points P of Fig. 14 are

$$P\left(\frac{S-1}{4O_1S}f_2, \frac{S}{2O_2}f_2\right).$$

Assuming that the curve between the jumping points is linear, the frequency variation corresponding to the free running frequency drift of 120 MHz is given by

$$\frac{\frac{S}{2Q_2}f_2}{\frac{S-1}{4O_1S}f_2} \times 120 \text{ MHz} = 2 \text{ MHz.}$$

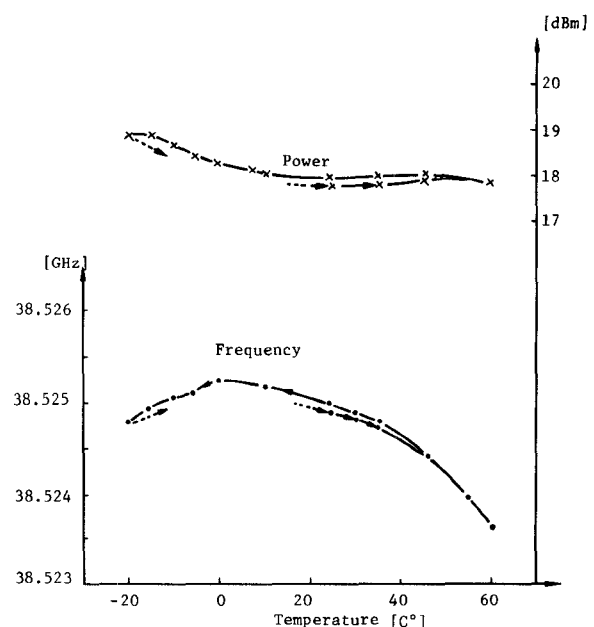


Fig. 15. Characteristics of frequency-stabilized IMPATT oscillator.

This value is of the same order as that of the obtained value. Fig. 15 also indicates an effect of the temperature compensated stabilizing cavity. The short brass section of the cavity piston opposes the expansion of the cavity made of invar iron.

Both of the sidebands produced by the amplitude modulation of the oscillating carrier are located far outside the pull-in range of the stabilized IMPATT diode oscillator, since the frequency of the bias modulation is 380 MHz and higher than the pull-in range.

Therefore, the stabilizing cavity has no effect on either sideband, and the only weighting of the sideband signals is provided by the tuning circuit of the original oscillator. At the same time no harmful effects of the bias modulation on frequency stabilization were detected.

The loaded Q of the original oscillator has the low value of 25, and the tuning characteristic is so wide that the amplitude and delay distortions of the sideband signals are negligible, because the frequency converted signal is a narrow band signal of 1.544 Mbit/s. The distortions are definite and can be equalized before modulation or after demodulation if necessary. Experimentally, no appreciable distortions were detected.

B. Frequency Conversion Characteristics

The frequency converted output power of the upper sideband is shown in Fig. 16 as a function of the applied IF signal power. The maximum output power without deformation of the output signal spectrum is +8.5 dBm in the case of +10 dBm IF input power when biased to 108 mA. The oscillator output power in case of bias modulation is +15 dBm. The conversion loss for the applied IF power is 1.5 dB. The temperature dependency of the frequency converted signal power is +8.5 dBm \pm 0.3 dB in the -20°C to $+60^{\circ}\text{C}$ range.

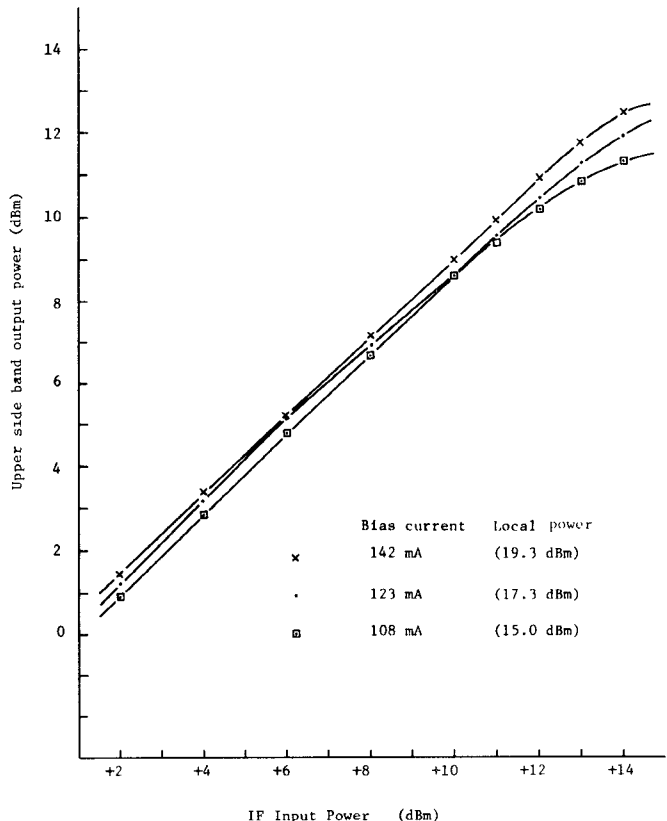


Fig. 16. Output power versus IF input power characteristic for frequency conversion.

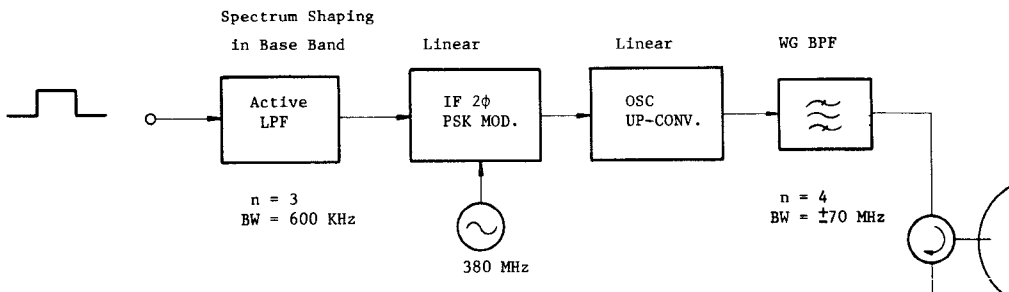


Fig. 17. Transmitting spectrum shaping considering FCC RR.

With regard to the up-conversion, the spectrum of the output signal should be limited to meet the FCC Rules and Regulations. Fig. 17 shows a flow path of the PCM signal to be transmitted. The waveguide filter in a millimeter-wave region can not restrict the spectrum of such a narrow-band signal of 1.544 Mbit/s. In the system, therefore, limitation of the radiation spectrum is performed in the baseband with a low-pass filter. The filter consists of an active filter of the order of $n=3$ of the feedback operational amplifier type; filter bandwidth is 600 kHz.

The functions of PSK modulation in the IF stage and up-conversion to 40 GHz are both designed to act on the linear portion of the input-to-output characteristics, so as not to produce distortion or spectrum broadening of the output signal.

The waveguide bandpass filter is a four-section Butterworth type with bandwidth of ± 70 MHz. This filter picks up the output signal and also acts to reject the unwanted radiation other than the transmitting sideband signal, and thus reflects the unwanted sideband signal to be absorbed by the isolator and the carrier signal to be fed to the receiving mixer.

Fig. 18(a) shows the signal spectrum at the output of the IF modulator. Fig. 18(b) indicates the up-converted signal spectrum in the 40-GHz band measured on the spectrum analyzer of HP-8555A (RF section).

The deformation or broadening of the spectrum due to nonlinearity of the IF input versus RF output characteristic of the self-oscillating up converter is observed below the -40 -dB level of the main output spectrum. These,

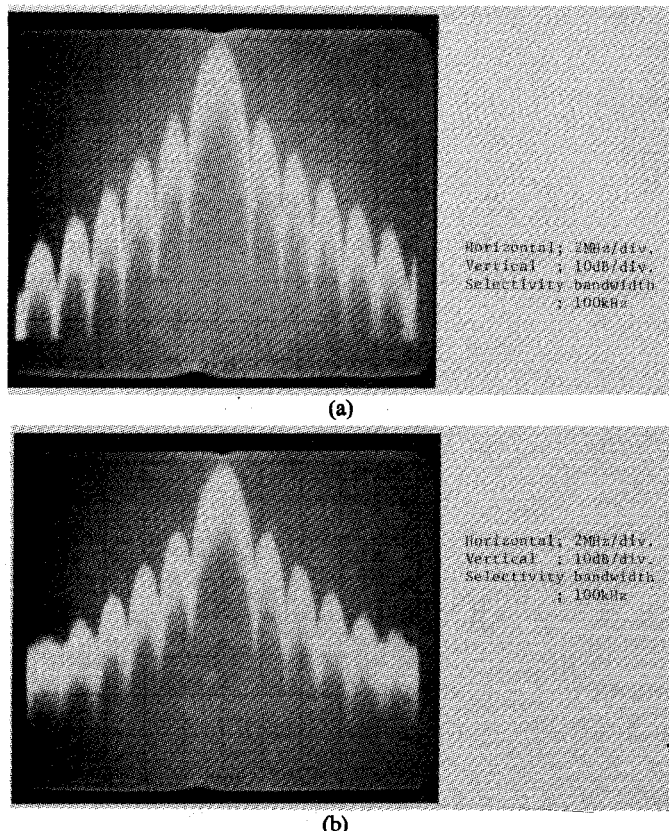


Fig. 18. (a) IF output spectrum with BB LPF. (b) RF output spectrum up-converted to 40 GHz.

however, are tolerable according to the FCC Rules and Regulations.

The FCC's emission limitations are given by the following equation:

$$A \text{ (dB)} = 11 + 0.4 (P - 50) + 10 \log B_A \quad (6)$$

where A (dB) is the attenuation of radiation power in 1-MHz bandwidth for the output power of the transmitter measured at the frequency differing by P percent of the authorized bandwidth B_A from the center frequency of transmitter. Attenuation A (dB), however, is not required within the authorized bandwidth, i.e., $A = 0$ for $P < 50$ and does not exceed 56 dB, $A \leq 56$.

The power spectrum distribution $S(f)$ from the carrier frequency for the two-phase PSK signal modulated by a random NRZ (Non Return to Zero) pulse code signal is given by the next equation:

$$S(f) = \left\{ \frac{\sin \pi f T}{\pi f T} \right\}^2 \quad (7)$$

where T is the pulse duration of a single code length. The occupied bandwidth B_o of 99-percent power of the filtered signal for this case is

$$B_o = 1.38 \times 1.544 \text{ MHz (clock rate)} \times 2(\text{both sidebands}) \\ = 4.26 \text{ MHz.}$$

The necessary bandwidth B_N is given by

$$B_N = \frac{2RK}{\log_2 S}$$

where

$$S \text{ number of code states; } \\ R \text{ maximum transmission speed (bits/s); } \\ K \text{ constant.}$$

In this case, constant K is determined to be 3.2 considering filter design and frequency drift of 2 MHz of the oscillator. Thus we obtain $B_N \approx 10$ MHz ($R = 1.544$ Mbit/s, $S = 2$, $K = 3.2$). The authorized bandwidth B_A for this case is 10 MHz, since the necessary bandwidth is larger than the occupied bandwidth.

Fig. 19 shows the measured spectrum radiation of the transmitter and also shows the emission limitation for the case of $B_A = 10$ MHz. In the figure, the maximum frequency drift of both the IMPATT diode oscillator and the transmitting IF oscillator is taken into account.

C. Effects on NF of Receiver

The mixer of the receiver is the waveguide-mounted planar type. The mixer diode is a silicon Schottky barrier diode of approximately 10- μ diameter (MX-40(R), OKI). The typical conversion loss of the RF mixer at 39 GHz is 6 dB with the local signal power of 7 dBm and without dc bias.

The pre-amplifier is constructed with two-stage transistor amplifiers and the gain and NF are 24 dB and 2 dB, respectively. The amplitude characteristic varies less than 0.2 dB in a bandwidth of 20 MHz.

In the radio system, the IMPATT diode oscillator is also used as the receiver local source. There are two main factors which degrade the noise characteristics of the mixer. One is the intrinsic noise of the IMPATT diode oscillator and the other is the modulation noise produced by the higher order nonlinear terms of the conductance variation due to the bias modulation.

Without use of a waveguide filter in the mixer local arm, the NF of the receiver was degraded by 6 dB as compared with the case of an external clean Gunn local source. The degradation was improved by providing the waveguide filter L BPF, which attenuates by more than 45 dB at the frequency of 320 MHz (=IF frequency) apart from the oscillating frequency. The filter is a four-section waveguide BPF with 3-dB bandwidth of 140 MHz. From experimentation it can be deduced that the principal factor which degrades the NF is the noise accompanying the local signal.

The other factor due to modulation was examined by measuring the receiver NF for both cases with and without bias modulation. The degradation of the NF due to the modulation was about 0.1 dB for the case with the waveguide filter as mentioned above, although the higher even-order terms, such as the 4th, 6th, 8th, etc., of the power series expansion of the conductance produce modulation noise around the oscillator signal. It was ascertained that the NF degradation due to the bias modulation was small as long as the up-converter was operated in the range of almost linear input-output characteristic.

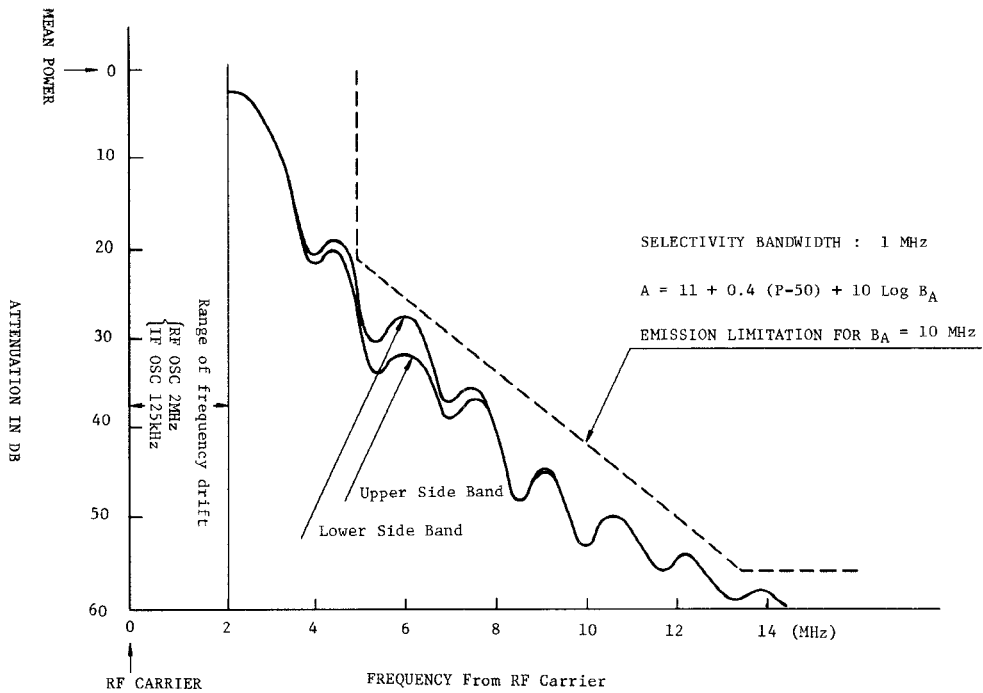


Fig. 19. Measured radiation spectrum and emission limitation.

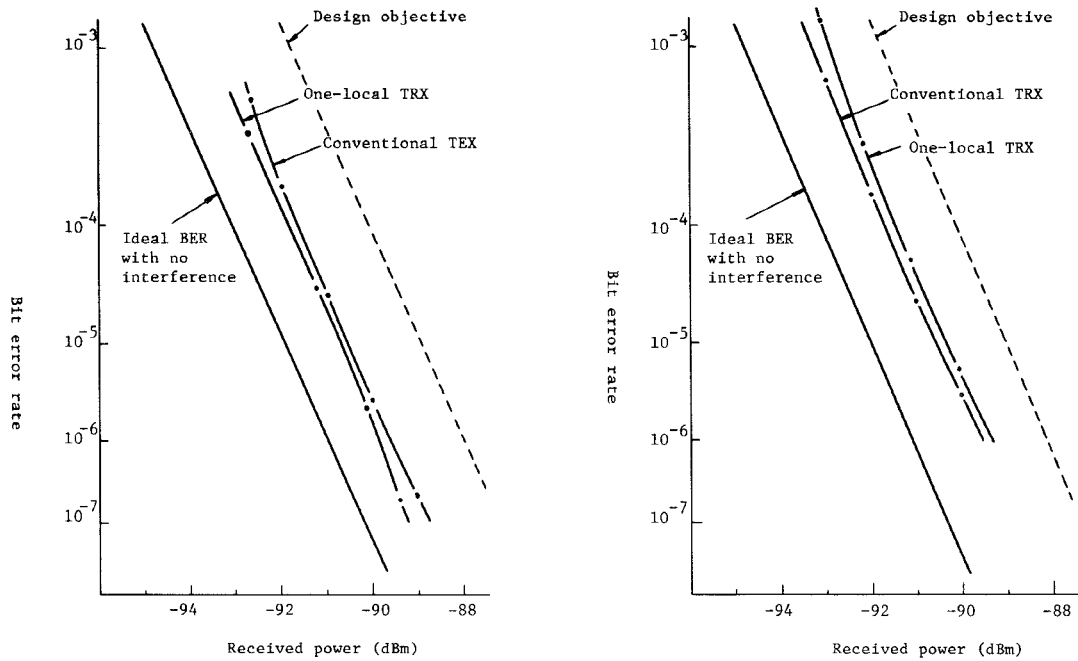


Fig. 20. (a) Transmitter quality. (b) Receiver quality.

The value obtained for the mixer NF was less than 8 dB including the IF pre-amplifier of NF 2 dB. The total NF determined from the antenna is less than 12 dB including R_{BPF} loss of 2 dB, circulator and isolator losses of about 0.5 dB each, and waveguide loss of 0.5 dB.

V. BER CHARACTERISTIC

Fig. 20 (a) shows the measured bit error rate (BER) characteristic versus the receiving power for the single oscillator transceiver in comparison with the conventional

transmitter consisting of a separate varactor up-converter. The single oscillator transmitter has a slightly better performance (0.2–0.3 dB better). This is considered to be due to the low distortion of the modulated PCM signal attributable to the circuit simplicity and wide band characteristics of the IMPATT diode oscillating up-converter.

On the other hand, Fig. 20 (b) shows the comparison of the measured BER of the single oscillator receiver with that of the conventional receiver with separate Gunn local source. The single oscillator receiver shows a slight de-

TABLE I
PERFORMANCE CHARACTERISTICS OF EQUIPMENT

Radio Frequency Band	38.6 - 40.0 GHz
Bit Rate	1.544 Mb/s
Capacity	24 Telephone Channels
Modulation	Bi-phase PSK
Authorized Bandwidth	10 MHz
System Gain	177 dB
Antenna Gain	More than 40dB
Beam Width	1.2°
Output Power	+7 dBm
Frequency Stability	0.012%
Receiver Configuration	Double Superheterodyne
	1st IF 320 MHz
	2nd IF 70 MHz
Receiver Noise Figure	Less than 12 dB
Demodulation	Coherent detection
Power Consumption	50 W (DC-48V)
Weight	45 kg
Dimensions	50cm(H), 50cm(W), 58cm(D)

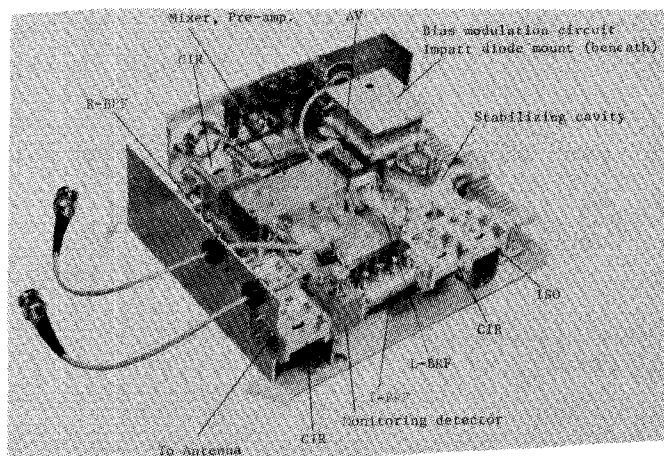


Fig. 21. 40-GHz single oscillator transceiver RF unit.

terioration of the order of 0.2 dB. This is considered to be due to the IMPATT local oscillator noise, although an RF BPF is provided in the local arm, and to the modulation noise.

These overall characteristics of the BER show that the single oscillator transceiver has performance comparable to the conventional transceiver, in spite of its simple circuit configuration.

VI. EQUIPMENT FEATURES

The outlines of the equipment are shown in Table I. The photograph of the RF unit of the single oscillator transceiver is shown in Fig. 21. The dimensions are 7 cm (H)×19 cm (W)×23 cm (D). The outside view of the equipment is shown in Fig. 22. The equipment is covered with a radome and comprises a 45-cm diameter parabolic

TABLE II
TYPICAL RAIN ATTENUATION AND FREE SPACE LOSS (REF. CCIR
REP. 721, FCC DOCKET 18920)

Free Space	Light Rain 2.5mm/H	Heavy Rain 12.5mm/H	Torrential 100mm/H
dB/km 124.8	1.0 dB/km	4.5 dB/km	23 dB/km

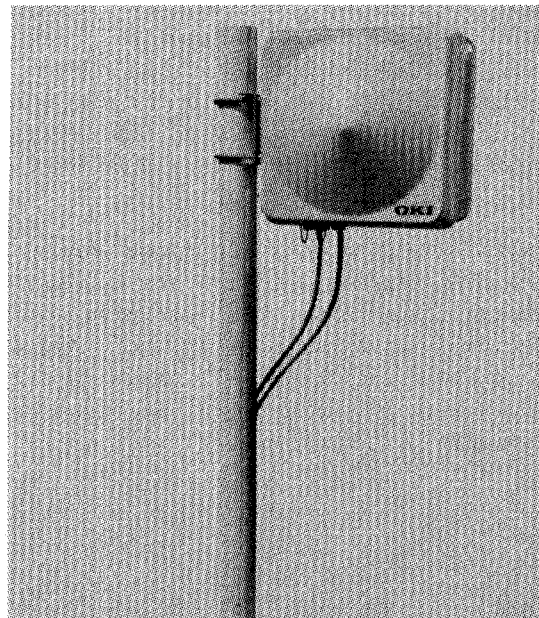


Fig. 22. Outside view.

antenna, transceiver units, and a voltage stabilizing unit. The cabinet can also house a hot standby redundant transceiver. The dimensions of the cabinet are 50 cm (H)×50 cm (W)×58 cm (D) and the weight of the complete equipment without the redundant system is about 45 kg.

The equipment is designed to be mounted on a pole of 4-in diameter on the roof or top of a building. By means of an attachment between the equipment and the pole, the direction of equipment can be adjusted vertically and horizontally.

The minimum receiving power required to obtain the BER of 10^{-3} is about -93 dBm, and -89 dBm for the BER of 10^{-6} , as shown in Fig. 20. Consequently, system gain G_s of this digital radio equipment amounts to about 100 dB (BER = 10^{-3}) for the output power of +7 dBm. Taking into account the antenna gain of more than 40 dB and a 2-dB loss margin for the waveguide feeder loss inside the cabinet and the radome loss on each side, the total gain is about 176 dB.

The maximum hop length is greatly dependent on the rainfall statistics of the area concerned and the required circuit reliability. Table II shows the free space loss and typical values for the rain attenuation in the 38.6–40-GHz band. Heavy rain of 12.5 mm/H is estimated to occur for 0.01–0.02 percent of the total time of the year in California.

VII. CONCLUSION

In conclusion, the single oscillator transceiver gave good performance. In spite of its simple circuit configuration, it had superior characteristics with regard to loss and distortion of the frequency up-conversion function as compared with conventional equipment having TX-local oscillator, an up-converter and a RX-local oscillator.

The waveguide circuits, which determine the equipment's cost, are greatly reduced, to about half those of the conventional equipment. Furthermore, the newly developed IMPATT diode mount with disk-hat type resonator provides stable operation and good adjustability.

The single oscillator transceiver is one solution to the problem of finding effective low-cost light-density local trunking radio equipment for intracity applications.

ACKNOWLEDGMENT

We would like to express our sincere thanks to Dr. S. Aoi and Y. Masuda, who gave the opportunity for research and development, and K. Kaminishi, who developed the semiconductor devices for this 40-GHz band radio equipment, and also to T. Iwano, H. Nakano, S. Endo, S. Gotoh, and Y. Fujita, who supported the development.

REFERENCES

- [1] P. T. Greiling and G. I. Haddad, "Large signal equivalent circuits of avalanche transit time devices," *IEEE Trans. Microwave Theory Tech.*, vol. MTT-18, pp. 842-853, Nov. 1970.
- [2] R. K. Gupta and C. G. Englefield, "Up-Conversion in IMPATT amplifiers," *IEEE Trans. Microwave Theory Tech.*, vol. MTT-26 pp. 28-30, Jan. 1978.
- [3] M. Hata, A. Fukasawa, M. Bessho, S. Makino, and M. Higuchi, "A new 40 GHz digital distribution radio with single local oscillator," *MTT-Int. Microwave Symp.*, B4.1, June 1978.
- [4] G. Cachier and J. Espagnol, "The pretuned module: An integrated millimeter wave oscillator," *ISSCC 77*, 11.7, 1977.
- [5] K. Nawata, "Studies on equivalent circuits of resonant-hat type IMPATT oscillators," *Trans. IECE (Japan)*, vol. J60-C no. 10, Oct. 1977.
- [6] K. Tajima, O. Kurita, and H. Suzuki, "Hat-type Impatt-diode amplifiers and their stabilization," *Microwave Meet. IECE Japan*, MW78-45, 1978.
- [7] K. Shirahata and K. Ogiso, "Stabilization of solid-state microwave oscillators by loading BPF," *Trans. IECE (Japan)*, vol. 54-B, no. 11, Nov. 1971.
- [8] T. Ohta and M. Hata, "Noise reduction of oscillators by injection locking," *Trans. IECE (Japan)*, vol. 53-B, no. 9, Sept. 1970.
- [9] W. J. Evans and G. I. Haddad, "Frequency conversion in IMPATT Diodes," *IEEE Trans. Electron Devices*, vol. ED-16, pp. 78-87, Jan. 1969.
- [10] H. Shiota, K. Kohiyama, and S. Kita, "A frequency stabilized self-oscillating converter using solid-state oscillators," *Trans. IECE (Japan)*, vol. J55-B, no. 12, pp. 691-692, Dec. 1972.

Practical Considerations in the Design of a High-Power 1-mm Gyromonotron

JOSEPH DOV SILVERSTEIN, MEMBER, IEEE, MICHAEL E. READ, KWO RAY CHU, AND ADAM T. DROBOT

Abstract—A second harmonic gyromonotron has been designed to have an output of 4 kW at a frequency of 240 GHz, and to operate with an overall efficiency of 14 percent. The design method utilized a detailed theory of the gyrotron oscillator and an electron orbit computer code. Particular attention was paid to the problem of mode competition in the oscillator cavity. Although a particular design example is considered, the method is of general interest.

I. INTRODUCTION

During the past several years the gyrotron [1] has been shown to be an efficient source (4-45 percent) of high-power radiation (1 kW-1 MW) at wavelengths less than 1 cm. Although a number of such devices have been

operated successfully in the U.S. in the 8-10-mm range, [2], [3], the only devices operating in the near-millimeter wave range ($\lesssim 3$ mm) are those built in the Soviet Union [4], [5].

This paper describes results of the design phase of the first known effort in the U.S. to build an efficient high-power gyrotron oscillator operating with a wavelength near 1 mm. Specifically, the design goals for this gyromonotron (i.e., single-cavity cyclotron resonance maser (CRM)) were 1-10 kW (peak) at 1.3. mm and an overall efficiency of 10-15 percent. It was to operate at the second harmonic of the cyclotron frequency ($\omega \approx 2\Omega_c$) and with a cavity mode of TE_{051} . Although these last two facts allow operation at reduced magnetic field and higher power than would be possible with the fundamental and lower order modes, they greatly increase the problem of mode competition; the circumvention of this complication is one of the main considerations in this design.

Manuscript received December 10, 1979; revised April 30, 1980.

J. D. Silverstein is with the U.S. Army Electronics Research and Development Command/Harry Diamond Laboratories, Adelphi, MD 20783.

M. E. Read, K. R. Chu, and A. T. Drobot are with the U.S. Naval Research Laboratory, Washington, D.C. 20375.